



A Journal of the Gesellschaft Deutscher Chemiker

Angewandte Chemie

GDCh

International Edition

www.angewandte.org

Accepted Article

Title: Synthesis of Porous Covalent Quinazoline Networks (CQNs) and Their Gas Sorption Properties

Authors: ONUR BUYUKCAKIR, Recep Yuksel, Yi Jiang, Sun Hwa Lee, Won Kyung Seong, Xiong Chen, and Rodney S. Ruoff

This manuscript has been accepted after peer review and appears as an Accepted Article online prior to editing, proofing, and formal publication of the final Version of Record (VoR). This work is currently citable by using the Digital Object Identifier (DOI) given below. The VoR will be published online in Early View as soon as possible and may be different to this Accepted Article as a result of editing. Readers should obtain the VoR from the journal website shown below when it is published to ensure accuracy of information. The authors are responsible for the content of this Accepted Article.

To be cited as: *Angew. Chem. Int. Ed.* 10.1002/anie.201813075
Angew. Chem. 10.1002/ange.201813075

Link to VoR: <http://dx.doi.org/10.1002/anie.201813075>
<http://dx.doi.org/10.1002/ange.201813075>

Synthesis of Porous Covalent Quinazoline Networks (CQNs) and Their Gas Sorption Properties

Onur Buyukcakir, Recep Yuksel, Yi Jiang, Sun Hwa Lee, Won Kyung Seong, Xiong Chen and Rodney S. Ruoff*

Abstract: The development of different classes of porous polymers by linking organic molecules using new chemistries still remains a great challenge. Here we introduce for the first time the synthesis of covalent quinazoline networks (CQNs) using an ionothermal synthesis protocol. Zinc chloride (ZnCl_2) was used as the solvent and catalyst for the condensation of aromatic *ortho*-aminonitriles to produce tricycloquinazoline linkages. The resulting CQNs show a high porosity with a surface area up to $1870 \text{ m}^2 \text{ g}^{-1}$. Varying the temperature and the amount of catalyst enables us to control the surface area as well as the pore size distribution of the CQNs. Furthermore, their high nitrogen content and significant microporosity make them a promising CO_2 adsorbent with a CO_2 uptake capacity of 7.16 mmol g^{-1} (31.5 wt %) at 273 K and 1 bar. Because of their exceptional CO_2 sorption properties, they are promising candidates as an adsorbent for the selective capture of CO_2 from flue gas.

The importance of porous materials has recently increased tremendously.^[1] Besides the well-studied zeolites and activated carbons, the metal-organic frameworks (MOFs) and porous organic polymers (POPs) have made a big impact on science and technology.^[2] There have been important advances in POPs and they have become an extensive class of porous materials.^[3] The adaptation of the synthesis strategies used in the synthesis of small organic molecules or conventional polymers has played an important role for the development of several porous polymers including covalent organic frameworks (COFs), conjugated microporous polymers (CMPs), porous aromatic frameworks (PAFs), hyper-crosslinked porous polymers (HCPs), polymers of intrinsic microporosity (PIMs), and covalent triazine frameworks (CTFs).^[4]

One of the important advances is the discovery of COFs by Yaghi and co-workers.^[5] COFs take advantage of dynamic covalent chemistry (DCC) by linking organic molecules by more strong covalent bonds than their metal-organic analogues. Although the first examples of COFs revealed a high crystallinity

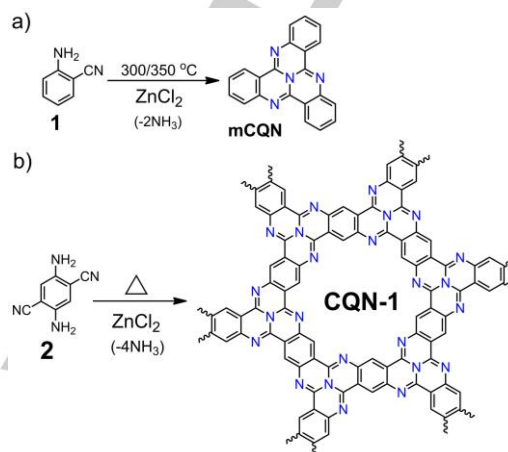


Figure 1. The synthesis route for covalent quinazoline networks (CQNs). a) Preparation of model compound, tricycloquinazoline (mCQN), b) The synthesis of CQN-1.

as well as a large surface area, they suffer from chemical and physical instability due to boron-containing linkages. The introduction of imine-linked COFs improved the stability considerably.^[6] In contrast, CTFs, which are a relatively new class of POPs reported by Thomas et al., were synthesized by an ionothermal reaction.^[7] The trimerization of aromatic nitriles in the presence of ZnCl_2 at high temperatures gives triazine-linked porous frameworks.^[8] Moreover, several other synthesis methods have been recently reported.^[9] The triazine linkage provides not only a high nitrogen content but also chemically and physically more stable porous polymers compared to COFs. Owing to their distinctive properties, they have been tested in diverse applications such as gas storage, separation, as catalysts or catalyst supports, and in energy storage.^[10] Although significant progress has been achieved for the preparation of POPs, the synthesis of new porous polymers is still of great interest. In this respect, the development of new linkages and synthesis strategies to produce polymers showing permanent porosity and large surface area, together with chemical and physical stability is greatly challenging but desirable. Here we introduce, for the first time, porous covalent quinazoline networks (CQNs) prepared by heating aromatic *ortho*-aminonitriles under ionothermal reaction conditions using ZnCl_2 as both a solvent and trimerization catalyst. This strategy also allows us to control the surface area as well as the pore size distribution of CQNs by simply changing the reaction temperature and the amount of ZnCl_2 . The tricycloquinazoline linkages serve not only as a nitrogen-rich polymeric network but also increase the physicochemical stability due to the presence of strong C-C and C-N bonds. The CQNs showed a high specific surface area up to $1870 \text{ m}^2 \text{ g}^{-1}$. In addition to their microporous texture, the high nitrogen content makes them promising CO_2 adsorption materials showing outstanding CO_2 uptake capacity at low pressures (up to 7.16 mmol g^{-1} , at 273 K and 1 bar) with a high CO_2/N_2 selectivity (up to 74.7).

Dr. O. Buyukcakir, Dr. R. Yuksel, Dr. Y. Jiang, Dr. S. H. Lee, Dr. W. K. Seong, Dr. X. Chen and Prof. Dr. R. S. Ruoff
Center for Multidimensional Carbon Materials (CMCM)
Institute for Basic Science (IBS)
Ulsan 44919 (Republic of Korea)
E-mail: rsuoff@ibs.re.kr, ruofflab@gmail.com

Prof. Dr. R. S. Ruoff
Department of Chemistry
Ulsan National Institute of Science and Technology (UNIST)
Ulsan 44919 (Republic of Korea)

Prof. Dr. R. S. Ruoff
School of Materials Science and Engineering
Ulsan National Institute of Science and Technology (UNIST)
Ulsan 44919 (Republic of Korea)

Supporting information for this article is given via a link at the end of the document.

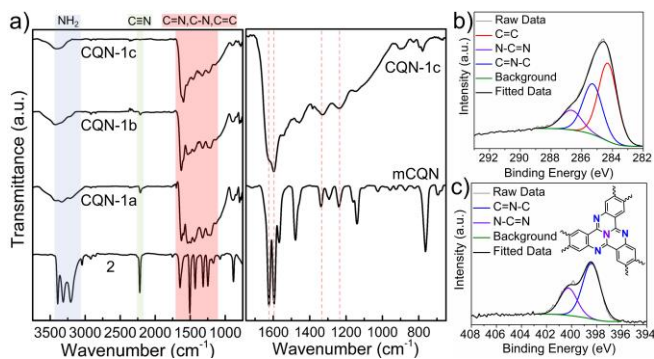


Figure 2. a) FTIR spectra of CQN-1(a-c) and compound 2 (left) and FTIR spectra of CQN-1c and mCQN (right). b) High resolution XPS C 1s spectrum of CQN-1c and c) N 1s spectrum of CQN-1c.

The CQNs were synthesized using the ZnCl₂ catalyzed ionothermal trimerization of aromatic *ortho*-aminonitrile monomers (Figure 1). In order to test the reaction feasibility and optimize the reaction conditions, tricycloquinazoline (mCQN) was selected as a model compound (Figure 1a). The mCQN was prepared by heating a mixture of compound 1 and one equivalent ZnCl₂ at 300 and 350 °C in flame-sealed ampoules to produce mCQN with 91 and 97% yields, respectively. In order to demonstrate the catalytic effect of the ZnCl₂ on the trimerization, a control experiment was conducted by heating the compound 1 in the absence of ZnCl₂ to yield *c*-mCQN. Crude ¹H-NMR analysis of the control samples treated at 300 and 350 °C showed respective yields of only 6 and 13% (see the Supporting Information (SI), Figure S10). This control reaction, therefore, indicates the large catalytic effect of the ZnCl₂ on the trimerization. In the same way, heat treatment of compound 2 (Figure 1b) in the presence of one equivalent ZnCl₂ at 300, 350 and 400 °C produced CQN-1a, CQN-1b and CQN-1c, respectively. In addition to the influence of reaction temperature on polymerization, the amount of ZnCl₂ has a significant effect on the structural features of the polymers. Hence, the impact of ZnCl₂ concentration was also investigated using five different salt/monomer mole ratios (1.0, 2.5, 5.0, 7.5 and 10) at 400 °C (Table 1). The resulting polymers were initially ground into fine powder and extensively washed with dilute HCl solution and water with the goal of removing ZnCl₂ residue. After washing, the CQNs were collected and dried under vacuum to give black colored fine powders in yields higher than 90 % (Table S1). Details of the synthesis and purification steps are given in the supporting information (SI).

The CQNs were investigated by Fourier-transform infrared spectroscopy (FTIR). The first indication of polymerization is the disappearance of *ortho*-aminonitrile related signals. While the carbonitrile bands around 2250 cm⁻¹ disappeared completely for CQN-1c, incomplete polymerization was noticed for CQN-1a and CQN-1b, that were synthesized at lower temperatures of 300 and 350 °C, respectively (Figure 2a, left). As seen in Figure S14, the increase of salt/monomer mole ratio from 1.0 to 2.5, 5.0, 7.5 or 10 leads to also the complete disappearance of the peaks associated with the carbonitrile moiety. Furthermore, the appearance of characteristic tricycloquinazoline vibrations signals (as observed for mCQN) at around 1625, 1595, 1335 and 1240 cm⁻¹ also indicates the successful trimerization of *ortho*-aminonitrile groups into tricycloquinazoline cores (Figure 2a, right). Solid-state cross-polarization magic angle spinning (CP/MAS) ¹³C NMR spectra of the CQNs confirmed the formation of tricycloquinazoline structures, where the resonance

observed at approximately 163 ppm can be assigned to the carbon atoms connected to nitrogen atoms in the tricycloquinazoline core (Figure S15). The other broad signals at 143, 125 and 108 ppm are assigned to aryl carbons. Like the FTIR analysis, the observed resonance signals belonging to carbon atoms attached to nitrile and amino moieties support the incomplete polymerization of CQN-1a and -1b.

The chemical bonding nature of CQNs was examined by X-ray photoelectron spectroscopy (XPS). The survey spectrum of CQNs revealed the presence of C 1s, N 1s and O 1s (Figure S16). The high-resolution C 1s spectrum of CQN-1c can be deconvoluted into three major peaks with binding energies 284.3, 285.3 and 286.8 eV (Figure 2b). The peak located at 284.3 eV can be assigned to carbon atoms in the aryl ring present in the skeleton (C=C). The peaks at 285.3 and 286.8 eV were attributed to the carbon atoms presents in the tricycloquinazoline core with C=N-C and N-C=N bonding, respectively. The N 1s spectrum denotes that there are two different nitrogen species with binding energies 398.3 and 400.4 eV, which can be respectively assigned to the nitrogen atoms located at the periphery (C=N-C) and the nitrogen atom located at the center (N-C=N) of the tricycloquinazoline core (Figure 2c).

The powder X-ray diffraction patterns of the CQN-1c showed two broad diffraction peaks at around 7° and 26°, signifying the existence of partial crystallinity but a lack of long-range ordering of the polymeric networks (Figure S17a). Because of the broadness of the peaks, it is difficult to acquire detailed information on structural order at the atomic level. However, the peak at 26° corresponds to the vertical spacing between stacked layers with a distance of about 3.4 Å. The peaks become broader with increasing ZnCl₂ concentration indicating the formation of less ordered structures (Figure S17b).

The particle morphology of the CQNs was studied using scanning electron microscopy (SEM). As shown in Figures 3 and Figure S18, CQNs showed monolithic morphologies with a size from several hundred nanometers to several microns. The formation of a porous network was verified using transmission electron microscopy (TEM), with the image shown in Figure 3c clearly showing the layered, microporous structure of CQN-1c. Elemental mapping by EDX indicated homogeneous distributions of carbon and nitrogen atoms in the skeletons of the CQNs (Figures 3e, 3f and S18).

The thermal stability of the polymeric networks was monitored using thermogravimetric analysis (TGA) by raising the temperature from room temperature to 900 °C at a rate of 10 °C min⁻¹ under a nitrogen atmosphere (Figure S19a). CQNs show excellent thermal stability up to 500 °C. The observed initial weight loss below 100 °C stemmed from mainly moisture

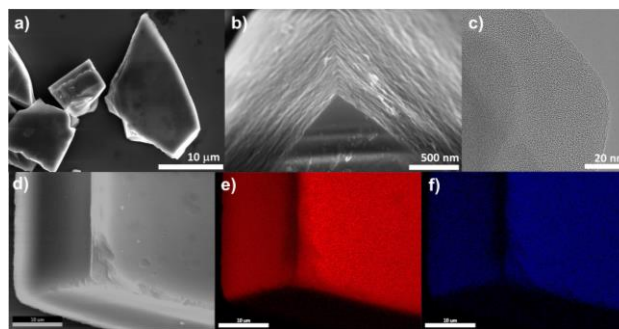


Figure 3. a), b) and d) SEM images of CQN-1c. c) TEM image of CQN-1c. e, f) elemental maps of CQN-1c for e) carbon f) nitrogen.

trapped inside the pores of CQNs. As also is typically observed for the CTFs prepared in ZnCl_2 salt melts,^[7,8a,b,e] some residual Zn metal salts ($\text{ZnCl}_2/\text{ZnOx}$) also remained inside the pores of our CQNs. In order to quantify any residual Zn metal salt, thermogravimetric analysis (TGA) was performed in air and less than 5.3 wt % residue was found (Figure S19b). The EDX spectra also verified the presence of Zn and Cl atoms (Figure S20) trapped inside the pores of CQNs. Elemental mapping by EDX showed an essentially homogeneous distribution of Zn and Cl atoms throughout the materials (Figure S18).

The elemental composition of each CQN was analyzed using X-ray photoelectron spectroscopy (XPS) survey analysis and elemental analysis by combustion (Table S1). Elemental analysis revealed a small deviation from the ideal C, H, and N values and this is primarily due to trapped water molecules and trapped Zn metal salt, as also shown by thermogravimetric and EDX analysis. The C/N ratio of CQNs also shows a slight deviation from the ideal C/N ratio, which is likely due to partial carbonization as well as the presence of unreacted terminal groups due to incomplete polymerization. Note that the increasing ZnCl_2 /monomer ratio does not lead to a notable change in the C/N ratio (that ranges from 3.12 to 3.19, close to the ideal value of 3.00).

The porosity of the CQNs was determined using nitrogen adsorption-desorption isotherms measured at 77 K (Figure 4a) which showed type I reversible sorption profiles. The steep nitrogen uptake at low relative pressures (below 0.01) indicated their microporous nature. The specific surface areas and pore size distributions were calculated using the Brunauer-Emmett-Teller (BET) and Non-Local Density Functional Theory (NLDFT), respectively. The BET specific surface areas of CQN-1a and -1b were measured as only $229 \text{ m}^2 \text{ g}^{-1}$ and $328 \text{ m}^2 \text{ g}^{-1}$, respectively. On the other hand, increasing the temperature to 400 °C increases the surface area of CQN-1c to $664 \text{ m}^2 \text{ g}^{-1}$. This observed substantial increase implies the formation of more extended networks compared to the incomplete polymerization of CQN-1a and 1b. Furthermore, to gain insight into the impact of the salt to monomer ratio on the porosity of the CQNs, five different ZnCl_2 /monomer mole ratios (1.0, 2.5, 5.0, 7.5 and 10) were also analyzed. The increasing concentration of ZnCl_2 leads to an increase in the surface area of the CQNs. CQN-1g had the highest surface area $1870 \text{ m}^2 \text{ g}^{-1}$ along with a pore volume of $0.93 \text{ cm}^3 \text{ g}^{-1}$. As previously observed for the CTFs,^[11] the use of higher amounts of ZnCl_2 up to a certain ratio leads to an increase in both surface area and pore volume by inducing the formation of more amorphous structures having a lower density than the long-range ordered networks. The pore size distributions (Figure 4b) show that all CQNs are predominantly microporous and the increasing ZnCl_2 concentration leads to not only an increase in microporosity but also contributes a mesoporosity to the networks. Detailed porosity values are given in Table 1. The results suggest that the surface area and pore size distributions of CQNs can be tuned easily by changing the synthesis temperature and the amount of ZnCl_2 used.

The earth's growing population together with its increasing energy demands has increased the combustion of fossil fuels, which is seen as the main source of the anthropogenic CO_2 emission.^[12] In this respect, the technologies for the selective capture of CO_2 from sources such as flue gas have become more crucial in reducing this now increasing CO_2 concentration.^[13] Current CO_2 capture methods use amine scrubbing technologies and suffer from high regeneration energy

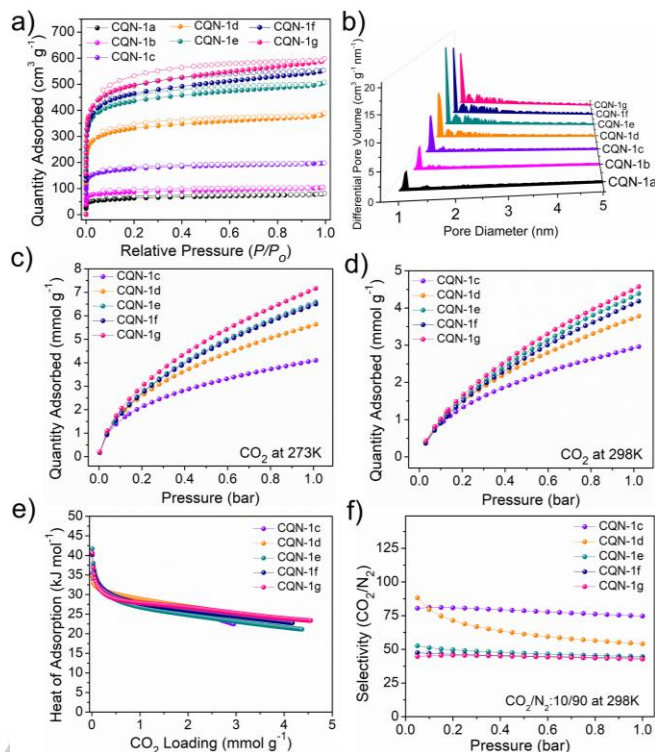


Figure 4. Gas sorption properties of the CQNs. a) N_2 adsorption-desorption isotherms of CQNs measured at 77 K b) Pore size distributions of CQNs calculated from N_2 isotherms using NLDFT. CO_2 adsorption isotherms of CQNs collected up to 1 bar at c) 273 K, and d) 298 K. e) The calculated Q_{st} of CQNs for CO_2 . f) The calculated CO_2/N_2 selectivity of CQNs at 298 K under flue gas conditions ($\text{CO}_2/\text{N}_2:10/90 \text{ v/v}$) using IAST.

penalties, degradation, and corrosive effects. Therefore, physisorptive CO_2 adsorbents like POPs are seen as a promising alternative by virtue of their low heat of adsorption and light elemental composition (C, H, N, O, S, and B).^[8b-d, 14] Even though many POPs have been tested for CO_2 capture and separation by simulating flue gas conditions, the exploration of new structures is needed. To this end, we have investigated the CO_2 capture and separation capability of CQNs.

As shown in Figures 4c and 4d, the CO_2 adsorption isotherms show that CQNs showed outstanding CO_2 uptake capacity at 273 K and 298 K up to 1 bar. Because of its highest surface area, CQN-1g exhibits the highest CO_2 uptakes of 7.16 mmol g^{-1} (31.5 wt % at 273 K and 1 bar) and 4.57 mmol g^{-1} (20.1 wt % at 298 K and 1 bar). The CO_2 uptakes of CQN-1g at 0.10 bar, corresponding to the partial pressure of CO_2 in the flue gas, are 2.04 and 1.03 mmol g^{-1} at 273 and 298 K, respectively. It is worth mentioning that to the best of our knowledge CQNs showed the highest CO_2 uptake values compared with previously reported POPs (Table S2). The CO_2 adsorption efficiency is closely related to pore size and heteroatom functionalities. Although there are debates underway about the role of nitrogen functionalities on CO_2 uptake capacity, the interactions between CO_2 molecules and N-containing functionalities also contribute to the CO_2 adsorption at some level.^[15] In this sense, this exceptionally high CO_2 uptake of CQNs can be attributed to their affinity to CO_2 molecules stemming from the synergetic effects of a high microporosity (0.90 -1.10 nm) with the high nitrogen content (up to 24 wt %) of the networks. In order to evaluate the CO_2 affinity, the heat of adsorption (Q_{st}) of CQNs for CO_2 was calculated from CO_2 isotherms measured at three different temperatures (273, 283,

Table 1. Gas sorption properties of CQNs prepared at different temperatures and ZnCl₂ concentrations.

CQNs	Temp. [°C]	ZnCl ₂ Eq.	S _A BET ^[a] [m ² g ⁻¹]	S _A Lang ^[b] [m ² g ⁻¹]	V _{Total} ^[c] [cm ³ g ⁻¹]	S _A Micro ^[d] [m ² g ⁻¹]	CO ₂ at 273K ^[e] [mmol g ⁻¹] (wt %)	CO ₂ at 298K ^[e] [mmol g ⁻¹] (wt %)	Q _{st} for CO ₂ ^[f] [kJ mol ⁻¹]	CO ₂ /N ₂ ^[g] Selectivity
CQN-1a	300	1.0	229	279	0.13	122	-	-	-	-
CQN-1b	350	1.0	328	386	0.16	234	-	-	-	-
CQN-1c	400	1.0	664	779	0.31	480	4.10 (18.0)	2.96 (13.0)	35.5	74.7
CQN-1d	400	2.5	1249	1467	0.60	891	5.63 (24.8)	3.78 (16.6)	34.6	54.1
CQN-1e	400	5.0	1647	1931	0.79	1190	6.58 (29.0)	4.39 (19.3)	41.7	44.6
CQN-1f	400	7.5	1749	2068	0.86	1183	6.50 (28.6)	4.18 (18.4)	40.1	43.5
CQN-1g	400	10	1870	2213	0.93	1264	7.16 (31.5)	4.57 (20.1)	40.6	42.7

[a] The calculated BET surface areas of CQNs from N₂ adsorption isotherms (77 K) using the relative pressure ranges determined according to Rouquerol plots (Figure S21 and S22). [b] Langmuir surface area of CQNs. [c] Total pore volumes at $P/P_0=0.99$. [d] The micropore surface areas of CQNs calculated using t-plot analysis. [e] CO₂ uptake values of CQNs at 1 bar, the values in parentheses are the CO₂ uptakes at weight percent (wt %) at 1 bar. [f] The isosteric heat of adsorption of CQNs for CO₂ obtained from the CO₂ isotherms collected at 273, 283 and 298 K. [g] The CO₂/N₂ selectivity of CQNs at 298 K calculated using IAST for the gas mixture CO₂/N₂:10/90 (v/v).

and 298 K) using the Clausius–Clapeyron equation (Figure 4e). The CQNs show high Q_{st} values in the range of 35 to 43 kJ mol⁻¹ at zero loading and the high loading affinity stays between 21–23 kJ mol⁻¹. In addition to the Q_{st} values for CO₂ of CQNs that are in the range of a physisorptive adsorption mechanism (lower than 43 kJ mol⁻¹), the reversible CO₂ isotherms also suggest a physisorption process (Figure S23).

These findings have motivated us to investigate the CO₂/N₂ selectivities of CQNs by simulating flue gas conditions. The selectivities were calculated according to ideal adsorption solution theory (IAST) using CO₂ and N₂ isotherms measured at 298 K for a mixture of CO₂ and N₂ with a ratio of 10/90 (v/v) (Figure 4f). The CQN-1c exhibited the highest CO₂/N₂ selectivity of 74.7 at 1 bar whereas the COF-1g, which has the highest CO₂ uptake capacity, showed the lowest selectivity (40.6) (Table 1). Two of the parameters that affect the CO₂/N₂ selectivity is the higher polarizability and quadrupole moment of CO₂ molecules compared to N₂. This polarizability difference helps achieve a higher interaction between polar adsorbents and CO₂ molecules, and this affinity contributes to the CO₂/N₂ selectivity. Another important parameter is the pore size, which plays a dominant role in the selectivity by a molecular sieving effect. However, the kinetic diameter difference between CO₂ and N₂ molecules is about 0.34 Å and it is highly challenging to achieve such pore size control, especially in amorphous materials. Although CQNs are microporous and have a high CO₂ affinity, their pore size distribution does not allow for a perfect sieving mechanism. This clearly explains the lowering of the selectivity of CQNs with increasing surface area in which more N₂ molecules can be accommodated. However, the kinetics of adsorption should also be taken into consideration since the narrow pore size leads to a slow adsorption rate.

In summary, we have demonstrated for the first time the design and synthesis of covalent quinazoline networks (CQNs). In addition to their high chemical and thermal stability, they showed a surface area greater than 1800 m² g⁻¹ along with large pore volumes up to 0.93 cm³ g⁻¹. They also exhibited an excellent CO₂ uptake capacity of up to 7.16 mmol g⁻¹ at 273 K and 1 bar. Their high CO₂ affinity and microporous nature contribute to their high CO₂/N₂ selectivity up to 74.7 (298 K and 1 bar) under flue gas conditions. These results suggest that they are promising materials for gas adsorption and separation applications. Because of their characteristic structural and

functional features, we suggest that CQNs will attract great interest. The simple preparation of variable organic building blocks and the easy ionothermal polymerization strategy will help in the synthesis of new CQNs derivatives, which may also have uses as catalysts and energy storage materials.

Acknowledgements

This work is supported by IBS-R019-D1.

Keywords: • microporous • polymer • ionothermal • quinazoline • CO₂ capture

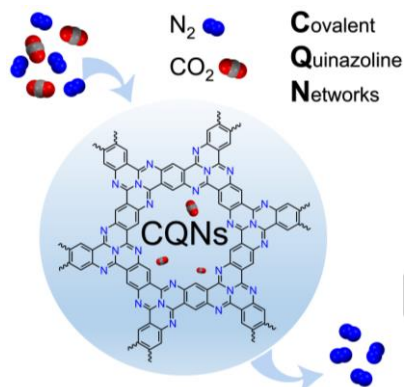
- [1] A. G. Slater, A. I. Cooper, *Science* **2015**, *348*, aaa8075.
- [2] a) M. R. Benzigar, S. N. Talapaneni, S. Joseph, K. Ramadass, G. Singh, J. Scaranto, U. Ravon, K. Al-Bahily, A. Vinu, *Chem. Soc. Rev.* **2018**, *47*, 2680–2721; b) X.-Y. Yang, L.-H. Chen, Y. Li, J. C. Rooke, C. Sanchez, B.-L. Su, *Chem. Soc. Rev.* **2017**, *46*, 481–558; c) H.-C. J. Zhou, S. Kitagawa, *Chem. Soc. Rev.* **2014**, *43*, 5415–5418; d) T.-H. Chen, I. Popov, W. Kaveevitvachai, O. Š. Miljanić, *Chem. Mater.* **2014**, *26*, 4322–4325.
- [3] a) P. Kaur, J. T. Hupp, S. T. Nguyen, *ACS Catal.* **2011**, *1*, 819–835; b) S. Das, P. Heasman, T. Ben, S. Qiu, *Chem. Rev.* **2017**, *117*, 1515–1563; c) D. Wu, F. Xu, B. Sun, R. Fu, H. He, K. Matyjaszewski, *Chem. Rev.* **2012**, *112*, 3959–4015.
- [4] a) A. I. Cooper, *Adv. Mater.* **2009**, *21*, 1291–1295; b) T. Ben, H. Ren, S. Ma, D. Cao, J. Lan, X. Jing, W. Wang, J. Xu, F. Deng, J. M. Simmons, S. Qiu, G. Zhu, *Angew. Chem. Int. Ed.* **2009**, *48*, 9457–9460; *Angew. Chem.* **2009**, *121*, 9621–9624; c) X. Zhu, C. Tian, T. Jin, J. Wang, S. M. Mahurin, W. Mei, Y. Xiong, J. Hu, X. Feng, H. Liu, S. Dai, *Chem. Commun.* **2014**, *50*, 15055–15058; d) L. Tan, B. Tan, *Chem. Soc. Rev.* **2017**, *46*, 3322–3356; e) M. Rose, N. Klein, I. Senkowska, C. Schrage, P. Wollmann, W. Böhlmann, B. Böhlinger, S. Fichtner, S. Kaskel, *J. Mater. Chem.* **2011**, *21*, 711–716; f) N. Keller, D. Bessinger, S. Reuter, M. Calik, L. Ascherl, F. C. Hanusch, F. Auras, T. Bein, *J. Am. Chem. Soc.* **2017**, *139*, 8194–8199; g) N. B. McKeown, P. M. Budd, *Chem. Soc. Rev.* **2006**, *35*, 675–683; h) O. Buyukcakir, S. H. Je, J. Park, H. A. Patel, Y. Jung, C. T. Yavuz, A. Coskun, *Chem. Eur. J.* **2015**, *21*, 15320–15327.
- [5] A. P. Côté, A. I. Benin, N. W. Ockwig, M. O’Keeffe, A. J. Matzger, O. M. Yaghi, *Science* **2005**, *310*, 1166–1170.
- [6] a) S. Kandambeth, A. Mallick, B. Lukose, M. V. Mane, T. Heine, R. Banerjee, *J. Am. Chem. Soc.* **2012**, *134*, 19524–19527; b) F. J. Uribe-Romo, J. R. Hunt, H. Furukawa, C. Klöck, M. O’Keeffe, O. M. Yaghi, *J. Am. Chem. Soc.* **2009**, *131*, 4570–4571; c) E. Vitaku, W. R. Dichtel, *J. Am. Chem. Soc.* **2017**, *139*, 12911–12914; d) H. Xu, J. Gao, D. Jiang, *Nat. Chem.* **2015**, *7*, 905–912.
- [7] P. Kuhn, M. Antonietti, A. Thomas, *Angew. Chem. Int. Ed.* **2008**, *47*, 3450–3453; *Angew. Chem.* **2008**, *120*, 3499–3502.
- [8] a) M. J. Bojdys, J. Jeromenok, A. Thomas, M. Antonietti, *Adv. Mater.* **2010**, *22*, 2202–2205; b) P. Katekomol, J. Roeser, M. Bojdys, J. Weber, A. Thomas, *Chem. Mater.* **2013**, *25*, 1542–1548; c) S. Hug, M. E. Tauchert, S. Li, U. E. Pachmayr, B. V. Lotsch, *J. Mater. Chem.* **2012**, *22*, 13956–13964; d) X. Zhu, C. Tian, G. M. Veith, C. W. Abney, J. Dehaut, S. Dai, *J. Am. Chem. Soc.* **2016**, *138*, 11497–11500; e) K. Schwinghammer, S. Hug, M. B. Mesch, J. Senker, B. V. Lotsch, *Energy Environ. Sci.* **2015**, *8*, 3345–3353; f) S. Kuecken, J. Schmidt, L. Zhi, A. Thomas, *J. Mater. Chem. A* **2015**, *3*, 24422–24427.

- [9] a) S. Ren, M. J. Bojdys, R. Dawson, A. Laybourn, Y. Z. Khimyak, D. J. Adams, A. I. Cooper, *Adv. Mater.* **2012**, *24*, 2357-2361; b) S. N. Talapaneni, T. H. Hwang, S. H. Je, O. Buyukcakir, J. W. Choi, A. Coskun, *Angew. Chem. Int. Ed.* **2016**, *55*, 3106-3111; *Angew. Chem.* **2016**, *128*, 3158-3163; c) E. Troschke, S. Grätz, T. Lübken, L. Borchardt, *Angew. Chem. Int. Ed.* **2017**, *56*, 6859-6863; *Angew. Chem.* **2017**, *129*, 6963-6967; d) K. Wang, L.-M. Yang, X. Wang, L. Guo, G. Cheng, C. Zhang, S. Jin, B. Tan, A. Cooper, *Angew. Chem. Int. Ed.* **2017**, *56*, 14149-14153; *Angew. Chem.* **2017**, *129*, 14337-14341; e) S.-Y. Yu, J. Mahmood, H.-J. Noh, J.-M. Seo, S.-M. Jung, S.-H. Shin, Y.-K. Im, I.-Y. Jeon, J.-B. Baek, *Angew. Chem. Int. Ed.* **2018**, *57*, 8438-8442; *Angew. Chem.* **2018**, *130*, 8574-8578.
- [10] a) N. Chaoui, M. Trunk, R. Dawson, J. Schmidt, A. Thomas, *Chem. Soc. Rev.* **2017**, *46*, 3302-3321; b) P. Puthiaraj, Y.-R. Lee, S. Zhang, W.-S. Ahn, *J. Mater. Chem. A* **2016**, *4*, 16288-16311.
- [11] a) P. Kuhn, A. Forget, J. Hartmann, A. Thomas, M. Antonietti, *Adv. Mater.* **2009**, *21*, 897-901; b) P. Kuhn, A. Forget, D. Su, A. Thomas, M. Antonietti, *J. Am. Chem. Soc.* **2008**, *130*, 13333-13337; c) P. Kuhn, A. Thomas, M. Antonietti, *Macromolecules* **2009**, *42*, 319-326.
- [12] R. S. Haszeldine, *Science* **2009**, *325*, 1647-1652.
- [13] a) M. Oschatz, M. Antonietti, *Energy Environ. Sci.* **2018**, *11*, 57-70; b) C. Xu, N. Hedin, *Materials Today* **2014**, *17*, 397-403; c) K. Sumida, D. L. Rogow, J. A. Mason, T. M. McDonald, E. D. Bloch, Z. R. Herm, T.-H. Bae, J. R. Long, *Chem. Rev.* **2012**, *112*, 724-781.
- [14] a) T. Islamoglu, S. Behera, Z. Kahveci, T.-D. Tessema, P. Jena, H. M. El-Kaderi, *ACS Appl. Mater. Interfaces* **2016**, *8*, 14648-14655; b) W. Lu, J. P. Sculley, D. Yuan, R. Krishna, Z. Wei, H.-C. Zhou, *Angew. Chem. Int. Ed.* **2012**, *51*, 7480-7484; *Angew. Chem.* **2012**, *124*, 7598-7602; c) V. Guillerm, Ł. J. Weseliński, M. Alkordi, M. I. H. Mohideen, Y. Belmabkhout, A. J. Cairns, M. Eddaoudi, *Chem. Commun.* **2014**, *50*, 1937-1940; d) N. Popp, T. Homburg, N. Stock, J. Senker, *J. Mater. Chem. A* **2015**, *3*, 18492-18504; e) G. Li, B. Zhang, Z. Wang, *Macromolecules* **2016**, *49*, 2575-2581; f) H. A. Patel, S. Hyun Je, J. Park, D. P. Chen, Y. Jung, C. T. Yavuz, A. Coskun, *Nat. Commun.* **2013**, *4*, 1357-1364; g) V. S. P. K. Neti, X. Wu, P. Peng, S. Deng, L. Echegoyen, *RSC Adv.* **2014**, *4*, 9669-9672; h) G. Wang, K. Leus, S. Zhao, P. Van Der Voort, *ACS Appl. Mater. Interfaces* **2018**, *10*, 1244-1249.
- [15] B. Adeniran, R. Mokaya, *Chem. Mater.* **2016**, *28*, 994-1001.

Entry for the Table of Contents

COMMUNICATION

A new class of porous organic polymers: Porous covalent quinazoline networks (CQNs) are designed and synthesized for the first time. CQNs have high surface area and microporosity with chemical and thermal stability. They show outstanding CO₂ adsorption capacity up to 31.5 wt % at low pressures.



Onur Buyukcakir, Recep Yuksel, Yi Jiang, Sun Hwa Lee, Won Kyung Seong, Xiong Chen, and Rodney S. Ruoff*

Page No. – Page No.

Synthesis of Porous Covalent Quinazoline Networks (CQNs) and Their Gas Sorption Properties

Accepted Manuscript